Scientific Research Publishing

Modern Mechanical Engineering, 2023, 13, 63-76
https://www.scirp.org/journal/mme
ISSN Online: 2164-0181
ISSN Print: 2164-0165

Simulation of the Behaviour Laws in the Thermal Affected Zones of the 13Cr-4Ni Martensitic Stainless Steel

Marcel Julmard Ongoumaka Yandza*, Harmel Obami-Ondon, Christian Tathy

Laboratory of Mechanics, Energetics and Engineering, Higher National Polytechnic School, Marien Ngouabi University, Brazzaville, Republic of Congo
Email: *julmard.marjus@gmail.com

How to cite this paper: Yandza, M.J.O., Obami-Ondon, H. and Tathy, C. (2023) Simulation of the Behaviour Laws in the Thermal Affected Zones of the 13Cr-4Ni Martensitic Stainless Steel. *Modern Mechanical Engineering*, **13**, 63-76.
https://doi.org/10.4236/mme.2023.134005

Received: August 5, 2023
Accepted: September 15, 2023
Published: September 18, 2023

Abstract

During the welding, many phenomena occur. The materials deform under the action of residual stresses. This tendency is due to the high gradients of temperature during the process. These deformations are really difficult for many professionals operating in the area. In the goal to predict these variations, one has established the behaviour laws which will be applied to evaluate residual stresses and strains. This research is focused on the study of the Thermal Affected Zone (TAZ) during the welding of the 13Cr-4Ni martensitic stainless steel. The TAZ does not know any change of state (solid/liquid). It only knows the metallurgical phase change (austenite/martensite). There are three types of behaviour laws in this study: thermal, mechanical and metallurgical behaviour laws. The thermal behaviour law serves to evaluate the temperature field which induces the mechanical strains. The mechanical behaviour law serves to evaluate spherical stress (pressure) and deviatoric stress which compose the residual stress. It also helps to measure the total strain. The metallurgical behaviour law serves for the evaluation of the metallurgical phase proportions. To validate the modelling developed in this study, one has made the simulations to compare the results obtained with the analytical and experimental data.

Keywords

Behaviour Laws, Martensitic Stainless Steel, Residual Stresses, Strain, Numerical Simulation

1. Introduction

Nowadays, the metallurgical industry is at its apogee. The steel materials are used

everywhere in the society. They serve in the transport for the fabrication of the cars. They are also used in many other systems and have a very large domain of applications. Between all these applications, there is the manufacture of the hydroelectric turbines. Many countries, like the Republic of Congo, need energy to stimulate their economic growth. The production of electricity, in the hydroelectric power station, depends on some parameters like the flow of water and the characteristics or the quality of the turbine.

So, thanks to its high corrosion resistance, the 13Cr-4Ni martensitic stainless steel is used for the fabrication of hydroelectric turbines [1]. Building turbines is an extremely complex task. The first reason is based on their particular geometries. The second one is associated with the welding process. During the welding, under the influence of the high gradients of temperature, the steel structures deform [2]. Welding residual stresses and deformations affect many mechanical properties of welded structures, such as fatigue performance, stiffness, and compressive stability. In addition, welding deformation is unfavorable to the fabrication accuracy and dimensional stability of welded structures [3]. The created strains resulting from residual stresses are permanent and need to be predicted to ensure the quality of the final product. So, the necessity to have good software to support the industrialists in their duties is crucial. Therefore, to create this software, one needs to model the equations which interpret the behaviour laws of the 13Cr-4Ni stainless steel during the welding. This modelling represents the central point of this article.

In the modelling section, one will first establish the thermal behaviour law to get the temperature field which exercises on the steel. Second, one will also make the mechanical behaviour law to evaluate the strains and residual stresses under the temperature field. Third, one will present the metallurgical behaviour law to determine the metallurgical phase proportions. The metallurgical phases (austenite/martensite) influence the mechanical behaviour of the welded pieces. To validate all these equations, one will compare the results of some simulations with the analytical and experimental data. All the simulations will be made by ANSYS 18.1 software. The study only focuses on the Thermal Affected Zones (TAZ). So, the change of state (solid/liquid) in the Fusion Zones (FZ) will not be considered.

2. Properties of the 13Cr-4Ni Stainless Steel

2.1. Physical Properties

The 13Cr-4Ni is a martensitic stainless steel. This steel is very used for the manufacture of the hydroelectric turbines. The physical properties of 13Cr-4Ni are in **Table 1** [4].

2.2. Chemical Composition

The chemical composition of the 13Cr-4Ni stainless steel, known by its industrial name S41500, is given in **Table 2** extracted from [5].

Table 1. Properties of 13Cr-4Ni stainless steel, extracted from [4].

Thermal properties			
Thermal dilatation	α	06 - 05 × 10^{-6}	K^{-1}
Thermal conductivity	k	17 - 78	$W{\cdot}m^{-1}{\cdot}K^{-1}$
Specific heat	c_p	450 - 460	$J{\cdot}Kg^{-1}{\cdot}K^{-1}$
Thermal diffusivity	α_s	2.34 × 10^{-5}	$m^2{\cdot}s^{-1}$
Melting temperature	T_f	1475	˚C
Density	ρ	1617 - 7241	$Kg{\cdot}m^{-3}$
Solidus	T_s	1400	˚C
Liquidus	T_l	1450	˚C
Resistivity	r	0.50 - 0.60	$\Omega{\cdot}mm^2{\cdot}m^{-1}$
Mechanical properties			
Tensile ultimate strength	R_u	750 - 950	MPa
Tensile yield strength	R_e	560 - 580	MPa
Elongation at break	R_p	18	pourcent
Young's modulus	E	206	GPa
Poisson's ratio	v	0.288	
Shear modulus	R_c	80	GPa

Table 2. Chemical composition of S41500 [5].

Weight by percentage	C	Mn	P	S	Si	Cr	Ni	Mo
S41500	0.034	0.68	0.018	0.001	0.44	12.7	4.0	0.57

3. Modelling of the Behaviour Laws

3.1. Thermal Behaviour Law

During the welding process, the welded pieces are under the effect of the high gradients of temperature. This phenomenon is not stationary in time. To determine the value of the temperature T at any point of the material, the heat unsteady Equation (1) is applied.

$$\rho c \frac{\mathrm{d}T}{\mathrm{d}t} = -div(q) + \dot{W} \tag{1}$$

with:

ρc : heat capacity;

$\frac{\mathrm{d}T}{\mathrm{d}t}$: temporal derivative of T;

q: heat flux;

$\dot{W}$: coupling term, internal heat source.

One also considers that the material obeys the isotropic conduction law. So, the heat flux is defined by the Fourier Law (2).

$$q = -kgrad(T) \tag{2}$$

with:

k: conductivity of the material.

To solve this equation, the conditions on the boundary $\partial\Omega = \partial\Omega_1 + \partial\Omega_2 + \partial\Omega_3$ are specified. Three (3) types of boundary conditions are distinguished (**Figure 1**):

1) Convective and radiative condition on $\partial\Omega_1$. To write mathematically this condition, the two types of heat transfer modes are united by (3).

$$-kgrad(T)\cdot n_{ext} = h(T_s - T_{ext}) \quad \text{with}: \begin{cases} h = h_{cv} + h_r \\ h_r = \varepsilon_r \sigma_r (T_s + T_{ext})(T^2 + T_{ext}^2) \end{cases} \tag{3}$$

T_{ext}, T_s: exterior temperature, temperature at the surface;

n_{ext}: exterior normal to the surface;

ε_r: emissivity;

σ_r: Stefan constant = 5.66961×10^{-8} kg·s^{-3}·K^{-4};

h, h_{cv}, h_r: global transfer coefficients, convection coefficient, radiation coefficient.

2) Dirichlet type condition with a set temperature $T = T_{imp}$ on $\partial\Omega_2$.

3) Or a Neumann type condition with a set flux such as $-kgrad(T)\cdot n_{ext} = \varphi_{imp}$ on $\partial\Omega_3$.

3.2. Mechanical Behaviour Law

The mechanical modelling consists of establishing a behaviour law on which the values of the strains and residual stresses can be calculated. The mechanical behaviour law must efficiently give in the TAZ the results near to the real solutions. It must be applied in a large range of temperatures.

To evaluate the total strain ε, its decomposition to the diverse natures of strain is made. The separation is done on the basis of physical phenomena which operate during the welding process. So, there are the: elastic strain ε^{el}, viscoplastic strain ε^{vp} and thermal strain ε^{th}.

In the literature like [6], for the study of the steels welding behaviour, they add the metallurgical dilation strain ε^{tr} (due to the dilation of pieces by the presence of the formed metallurgical phases) and the transformation plasticity strain ε^{pt} (due to the plasticity caused by the formed metallurgical phases). In this article, these two last types of strain are not considered because their influences are weak.

So, one can write the mechanical behaviour law such as (4):

$$\varepsilon = \varepsilon^{el} + \varepsilon^{vp} + \varepsilon^{th} \tag{4}$$

So, the different strains are:

3.2.1. Elastic Strain

The elastic strain is calculated by the Hooke Law:

$$\dot{\sigma} = E\dot{\varepsilon}^{el} = E^{-1}\dot{\sigma} + \dot{T}\frac{\partial E^{-1}}{\partial T}\sigma \tag{5}$$

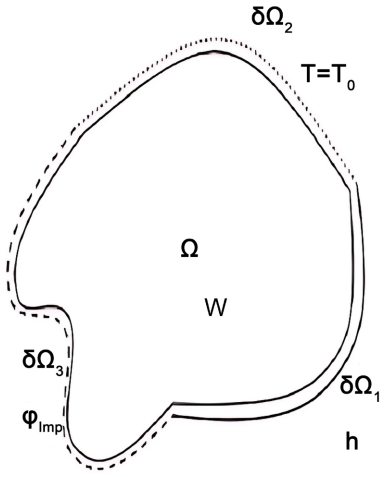

Figure 1. Boundary conditions of the thermal problem.

So, the equation of the elastic strain ε^{el} is such as:

$$\dot{\varepsilon}^{el} = \frac{1+\nu}{E}\dot{\sigma} - \frac{\nu}{E}tr(\dot{\sigma})\mathbf{I} + \dot{T}\frac{\partial}{\partial T}\left(\frac{1+\nu}{E}\right)\sigma - \dot{T}\frac{\partial}{\partial T}\left(\frac{\nu}{E}\right)tr(\sigma)\mathbf{I} \tag{6}$$

with:

ν : Poisson's ratio;

E: Young's modulus;

σ : stress.

By dividing the stress $\sigma = s - p\mathbf{I}$ to a deviatoric part s and a spherical one p (pressure), the following equations are obtained:

$$\dot{e}^{el} = \frac{\dot{s}}{2\mu} - \dot{T}\frac{1}{2\mu^2}\frac{\partial \mu}{\partial T}s \tag{7}$$

$$tr\left(\dot{\varepsilon}^{el}\right) = -\frac{\dot{p}}{\chi} + \dot{T}\frac{1}{\chi^2}\frac{\partial \chi}{\partial T}p \tag{8}$$

$\dot{e}^{el}$: deviatoric part of $\dot{\varepsilon}^{el}$;

μ : Lamé coefficient;

χ : hydrostatic compression modulus.

The Lamé coefficient μ and the hydrostatic compression modulus χ are given by:

$$\mu = \frac{E}{2(1+\nu)},$$

$$\chi = \frac{E}{3(1-2\nu)}.$$

3.2.2. Thermal Strain

To establish the thermal strain, the mass conservation Equation (9) is used.

$$tr(\dot{\varepsilon}) = tr\left(\dot{\varepsilon}^{th}\right) = \nabla \cdot v = -\frac{1}{\rho}\frac{\mathrm{d}\rho}{\mathrm{d}t} \tag{9}$$

And the thermal tensor ε^{th} is considered as spherical such as (10):

$$\dot{\varepsilon}^{th} = -\frac{1}{3\rho}\frac{\mathrm{d}\rho}{\mathrm{d}t}\mathbf{I} \tag{10}$$

The thermal strain rate is linked to the dilation coefficient α and the cooling speed $\dot{T}$ such as:

$$tr\left(\dot{\varepsilon}^{th}\right) = 3\alpha\dot{T}.$$

This leads to:

$$\dot{\varepsilon}^{th} = \alpha\dot{T}\mathbf{I} \tag{11}$$

3.2.3. Viscoplastic Strain

Perzyna [7] has defined a relation between the viscoplastic strain rate and the deviatoric stress *s* such as:

$$\dot{\varepsilon}^{vp} = \frac{\sqrt{3}}{2\bar{\sigma}}\left\langle\frac{\bar{\sigma}-\sigma_s}{K\sqrt{3}}\right\rangle^{1/m} s \tag{12}$$

$\langle x\rangle = x \quad \text{si} \quad x \geq 0$,

$\langle x\rangle = 0 \quad \text{si} \quad x \leq 0$.

K: material consistency;

m: sensibility of the thermal stress.

There is a viscoplastic flow when the Von Mises stress is higher than the flow threshold σ_s. The equivalent stress $\bar{\sigma}$ acts like a tensile stress. In the results section, Equation (13) is used to compare this stress with the tensile stress developed by the tensile test of a steel bar.

$$\bar{\sigma} = \sigma_s + K\dot{\bar{\varepsilon}}^{m(T)}\bar{\varepsilon}^{n(T)} \tag{13}$$

3.3. Metallurgical Behaviour Law

In the TAZ of the martensitic stainless steel 13Cr-4Ni, there are two phases: austenite during the heating and martensite during the cooling.

3.3.1. Austenitic Phase Proportion

To evaluate the austenitic phase proportion g_γ, W. Zhang [8] proposes the modified Avrami Equation (14).

$$g_\gamma = 1 - \exp\left(-k_0 s\right)^n \tag{14}$$

with:

$$s = \sum_{i=1}^{m_i}\exp\left(-\frac{E_a}{RT_i}\right)\Delta t_i,$$

E_a : transformation apparent activation energy;

k_0, n : parameters;

R: ideal gas constant;

T_i : temperature at initial instant t_i;

m_i : number of increments.

In this study, the values of these above cited parameters are given in **Table 3** like presenting by J.B. Levesque [5].

To validate the austenitic phase proportion g_γ, the results obtained will be compared with the experimental values found by J.B. Levesque [5].

3.3.2. Martensitic Phase Proportion

Van Bohemen *et al.* [9] have studied the influence of chemical composition on the martensitic phase proportion. They have proposed the Equation (15) to evaluate the martensitic phase proportion by using the chemical composition and the temperature.

$$g_{\alpha'} = 1 - \exp\left(-a_m\left(T_{KM} - T\right)\right) \tag{15}$$

with:

T_{KM} : temperature at the beginning of martensitic transformation;

a_m : parameter of transformation rate;

T: temperature of the material.

The authors have defined T_{KM} and a_m as follow:

$$T_{KM} = 462 - 273x_C - 26x_{Mn} - 16x_{Ni} - 13x_{Cr} - 30x_{Mo} \tag{16}$$

$$a_m = 0.0224 - 0.0107x_C - 0.0007x_{Mn} - 0.00005x_{Ni} - 0.00012x_{Cr} - 0.0001x_{Mo} \tag{17}$$

The chemical atom proportion x of the 13Cr-4Ni stainless steel, S41500, is given in **Table 2**. The values found by J.B. Levesque are used to make the comparison with the results of this study.

4. Results and Discussion

All the equations of the modelling section are implemented in ANSYS 18.1 software to get the results presented in this section.

4.1. Validation of the Mechanical Behaviour Law

4.1.1. Elasto-Viscoplastic Strain: Tensile Test

To validate or verify the correctness of the elasto-viscoplastic strain term in the mechanical behaviour law, the tensile test is made. As specified in Section 3.2.3, viscoplastic stress acts like tensile stress. So, the Von Mises equivalent stress (tensile stress) is given by (18).

$$\sigma_{eq} = \bar{\sigma} - \sigma_s = K\dot{\bar{\varepsilon}}^{m(T)}\bar{\varepsilon}^{n(T)} \tag{18}$$

By Equation (18), the analytical values are compared with the numerical ones found by the tensile test with ANSYS 18.1.

The physical parameters for the analytical calculus are given in **Table 4**.

The experimental traction device is made as follows: a cylindrical bar of initial length $l_0 = 50\,\text{mm}$ and radius $r_0 = 5\,\text{mm}$ is used. The device presents two boundary conditions. At the top, a vertical speed $V = 5\times10^{-6}\,\text{m}\cdot\text{s}^{-1}$ is applied. At the bottom, the bar is fixed as presented in **Figure 2**.

Table 3. Parameters of the simulation.

E_a	k_0	n
509.9 KJ·mol^{-1}	4.04×10^{24}	0.66

Table 4. Mechanical parameters of 13Cr-4Ni steel [4].

K (MPa·s^{-1})	m	n	σ_s (MPa)	ν	E (GPa)
252	0,3	0.35	20	0.288	206

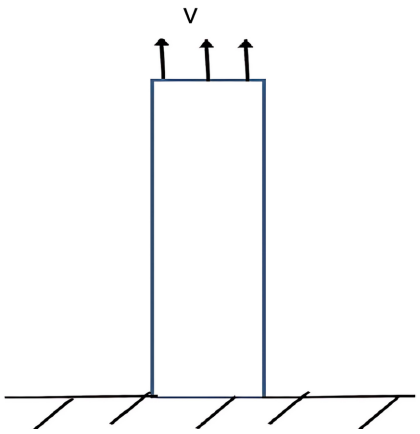

Figure 2. Geometry of the cylindrical bar in the tensile test.

The analytical and the numerical values of the experiment are presented in **Figure 3**.

By **Figure 3**, the numerical values are near to the analytical ones. So, the modelling conceived is correct.

4.1.2. Thermal Strain

To validate the expression of the thermal strain in the mechanical behaviour law, the thermal loading on ANSYS 18.1 is made. So, a cylindrical bar of length 0.1 m and 0.1 m of radius is used. A progressive heat source of temperature $T(t)$ variable in the time is applied. The Temperature increases by 5˚C·s^{-1}. The cylindrical bar is fixed between two trays. The experiment is done during $t = 20\,\text{s}$. The time step is $\Delta t = 0.1\,\text{s}$.

The analytical expression of thermal strain is given by (19).

$$\sigma^{th} = E\varepsilon^{th} = \alpha E\dot{T}t \tag{19}$$

Figure 4 shows the comparison between the analytical (gray) and the numerical values (orange) obtained. The results found are near. The coherence of results is found.

4.2. Validation of the Thermal Behaviour Law

Kondrashov [10] proposes an analytic solution of the heat equation for the non-isothermal transformations with a Neumann type condition. This solution

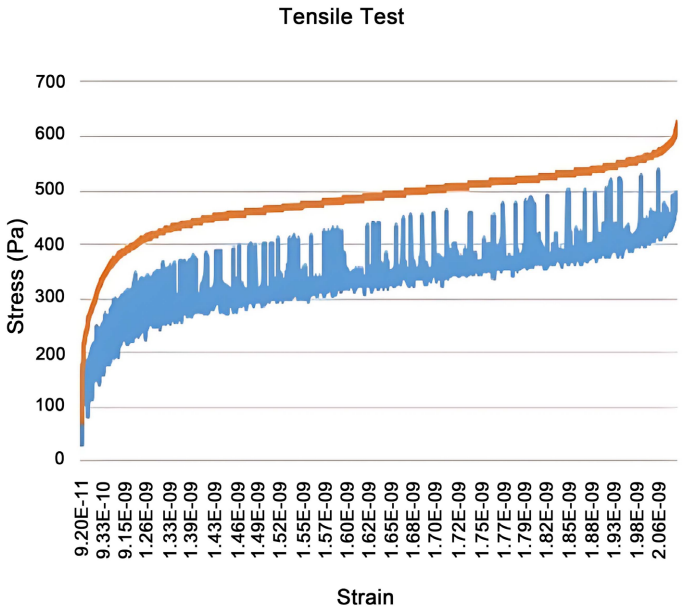

Figure 3. Tensile test, analytical results (orange), numerical results (blue).

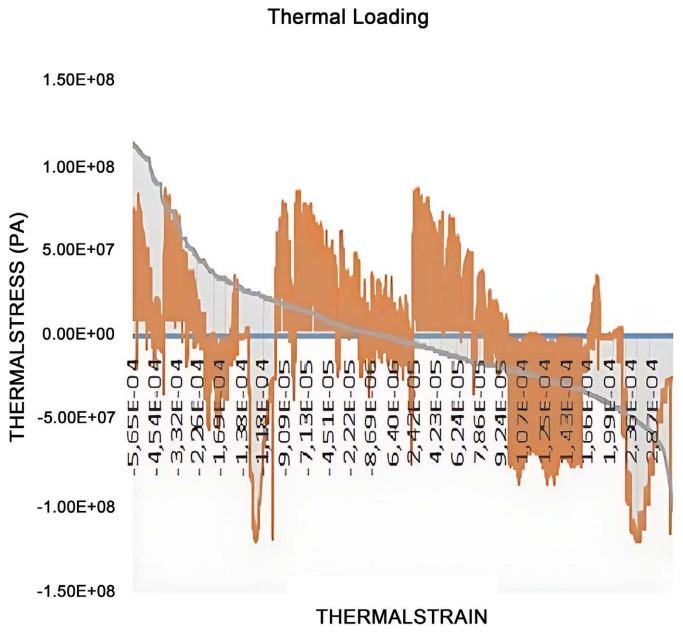

Figure 4. Thermal stress.

is used for comparing the numerical solution, implemented by ANSYS 18.1, with this analytic one. The analytic solution of the heat equation is given by (20).

$$T(x,t) = T_0 + (T_s - T_0)\frac{erf\left(\frac{x}{2\sqrt{\alpha_s t}}\right)}{erf\left(\frac{k_s}{2\sqrt{\alpha_s}}\right)} \tag{20}$$

with:

$$T(t=0)=T_i$$

$$T(x=0)=T_0$$

$$T(x=\infty)=T_i$$

$$T_s=T\left(x=x_s=k_s\sqrt{t}\right).$$

α_s : thermal diffusivity;

k_s : thermal conductivity;

x_s : solidus position or limit of the TAZ;

T_s : solidus.

$erf(X)$ is the Gauss error function. It is defined as follows:

$$erf(X)=\frac{2}{\sqrt{\pi}}\int_0^X \exp\left(-u^2\right)\mathrm{d}u \tag{21}$$

So:

$$erf\left(\frac{x}{2\sqrt{\alpha_s t}}\right)=\frac{2}{\sqrt{\pi}}\left(-\frac{x^2}{2\alpha_s t}+\frac{x}{2\sqrt{\alpha_s t}}-2\right)\exp\left(-\frac{x^2}{4\alpha_s t}\right)+\frac{4}{\sqrt{\pi}} \tag{22}$$

$$erf\left(\frac{k_s}{2\sqrt{\alpha_s}}\right)=\frac{2}{\sqrt{\pi}}\left(-\frac{k_s^2}{2\alpha_s}+\frac{k_s}{2\sqrt{\alpha_s}}-2\right)\exp\left(-\frac{k_s^2}{4\alpha_s}\right)+\frac{4}{\sqrt{\pi}} \tag{23}$$

To solve numerically the heat Equation (1), a 2D bar 1 × 50 mm^2 is considered. The initial temperature of the material is $T_i=1650^{\circ}\mathrm{C}$. The temperature at the left limit is suddenly reduced to 800˚C. The time step is $dt=0.1\,\mathrm{s}$ and the space step is $dx=dy=0.5\,\mathrm{mm}$. The simulation is made during $t=20\,\mathrm{s}$. **Figure 5** shows the profile of temperature in the bar during the simulation.

The analytic (black color) and numerical (blue color) results obtained are presented in **Figure 6**. The two results are numerically near. So, the correctness of the results is found.

4.3. Validation of the Metallurgical Behaviour Law

4.3.1. Martensitic Phase Simulation

On the basis of the metallurgical phase proportion modelling, the martensitic phase proportion is obtained. The curve presenting this evolution is given in **Figure 7**.

The numerical solution is compared with the experimental data found by J.B. Levesque [5]. The evolution of the experimental curve is given in **Figure 8**.

4.3.2. Austenitic Phase Simulation

The numerical austenitic phase proportion, found on the basis of the modelling developed in Section 3.3, is given in **Figure 9**.

The values found by the simulation are compared with the experimental data [5] (**Figure 10**). So, the correctness of the results is found.

5. Conclusion

In this article, the thermal, mechanical and metallurgical behaviour laws in the

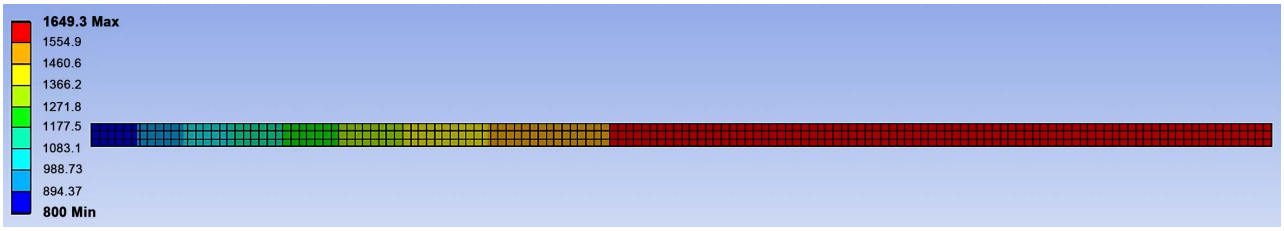

Figure 5. Temperature profile in the bar.

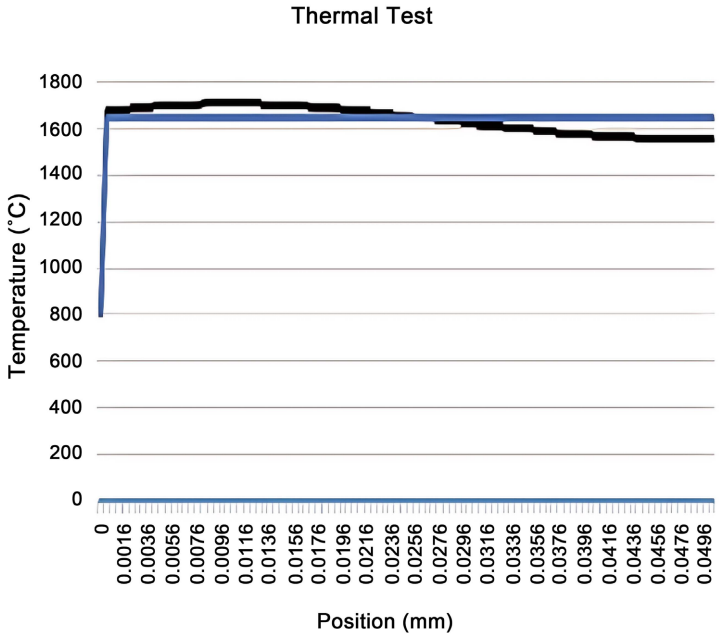

Figure 6. Analytical (black) and numerical (blue) results.

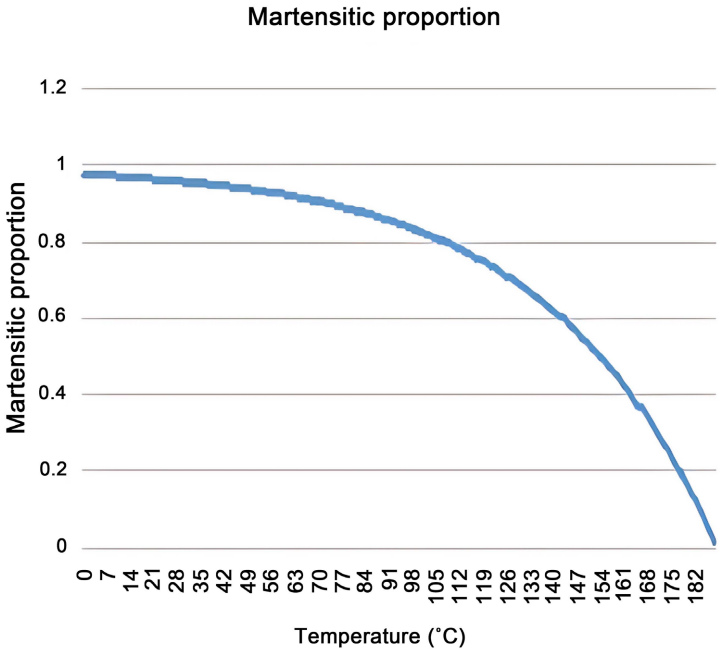

Figure 7. Martensitic phase proportion by numerical simulation.

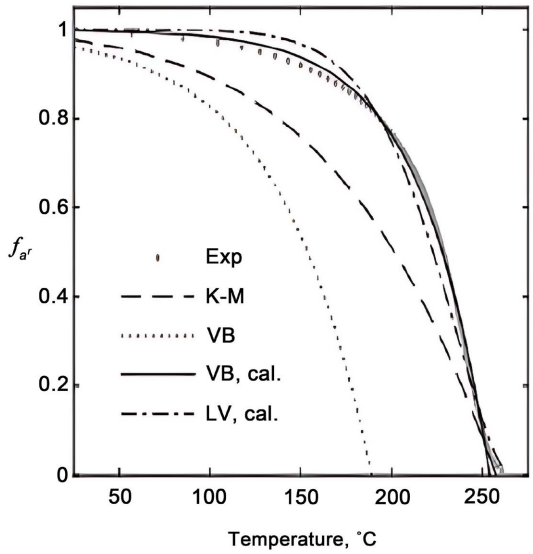

Figure 8. Martensitic phase proportion by experimental data extracted from [5].

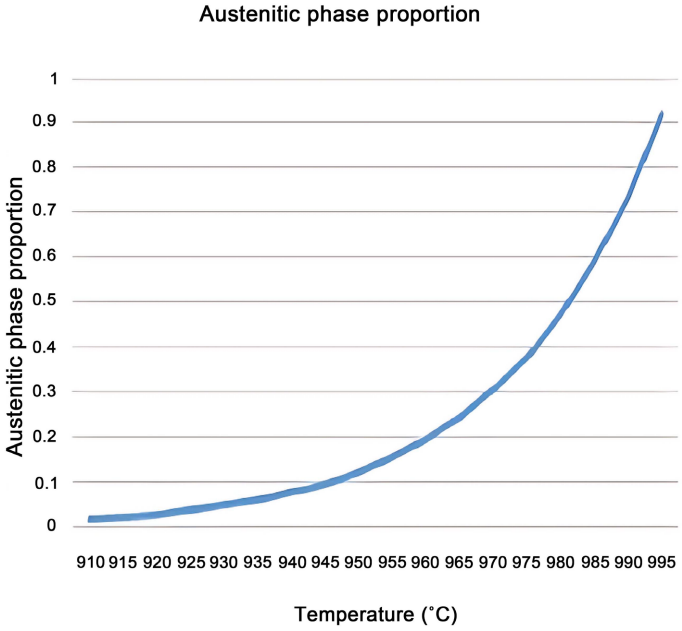

Figure 9. Austenitic phase proportion by numerical simulation.

TAZ of the 13Cr-4Ni stainless steel are presented. The mechanical behaviour law serves to evaluate the strains and residual stresses. So, to evaluate the stresses and the strains during the welding, some equations are developed. To validate these equations, one has confronted their numerical results with the analytic or experimental data. One has made the same for the thermal and metallurgical behaviour laws. The thermal modelling is based on the heat equation. The metallurgical behaviour law focuses on the solid-state phase proportions (martensite and austenite). The results obtained show the correctness of the modelling. The future research directions on the simulation of the welding must take into

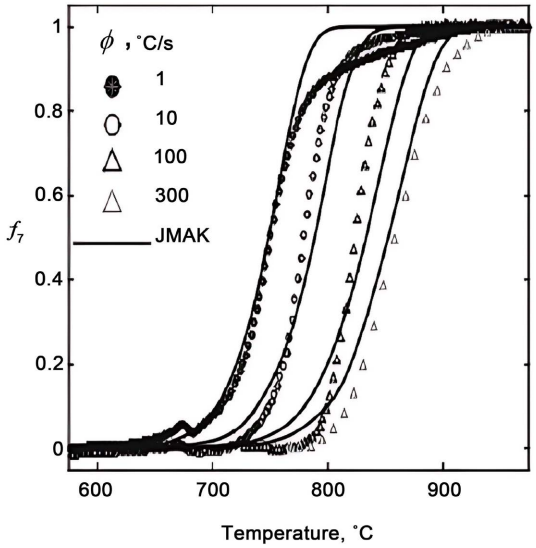

Figure 10. Austenitic phase proportion by experimental data extracted from [5].

account the prediction of the fissure formation. The fissuring is a real problem during the welding which influences the material stability.

Conflicts of Interest

The authors declare no conflicts of interest regarding the publication of this paper.

References

[1] Mc Guire, M. (2008) Stainless Steels for Design Engineers. ASM International, Materials Park, USA. https://www.asminternational.org

[2] De Sanctis, M., Lovicu, G., Buccioni, M., Donato, A., Richetta, M. and Varone, A. (2017) Study of 13Cr-4Ni-(Mo) (F6NM) Steel Grade Heat Treatment for Maximum Hardness Control in Industrial Heats. *Metals*, **7**, Article 351. https://doi.org/10.3390/met7090351

[3] Sonsimo, C.M. (2008) Effect of Residual Stresses on the Fatigue Behaviour of Welded Joints Depending on Loading Conditions and Weld Geometry. *International Journal of Fatigue*, **31**, 88-101. https://doi.org/10.1016/j.ijfatigue.2008.02.015

[4] Matweb (2023) Overview of Materials for Low Alloy Steel. https://www.matweb.com/search/datasheet

[5] Levesque, J.B., Lanteigne, J., Champliaud, H. and Paquet, D. (2020) Modeling Solid-State Phase Transformations of 13Cr-4Ni Steels in Welding Heat-Affected Zone, *Metallurgical and Materials Transactions A*, **51**, 1208-1220. https://doi.org/10.1007/s11661-019-05587-1

[6] Gautier, E. (1997) Interactions between Stresses and Diffusive Phase Transformations with Plasticity, In: Berveiller, M. and Fischer, F.D., Eds., *Mechanics of Solids with Phase Changes. International Centre for Mechanical Sciences*, Springer, Vienna, 105-120. https://doi.org/10.1007/978-3-7091-2660-8_4

[7] Heeres, O.M., Suiker, A.S.J. and de Borst, R. (2002) A Comparison between the Perzyna Viscoplastic Model and the Consistency Viscoplastic Model. *European Journal of*

Mechanics, **21**, 1-12. https://doi.org/10.1016/S0997-7538(01)01188-3

[8] Zhang, W., Elmer, J.W. and DebRoy, T. (2002) Modeling and Real Time Mapping of Phases during GTA Welding of 1005 Steel. *Materials Science and Engineering*: *A*, **333**, 320-335. https://doi.org/10.1016/S0921-5093(01)01857-3

[9] Van Bohemen, S.M.C. and Sietsma, J. (2009) Effect of Composition on Kinetics of Athermal Martensite Formation in Plain Carbon Steels. Materials Science and Technology, **25**, 1009-1012. https://doi.org/10.1179/174328408X365838

[10] Kondrashov, E.N. (2009) The Analytical Solution of the One Alloy Solidification Problem. *International Journal of Heat and Mass Transfer*, **52**, 67-69. https://doi.org/10.1016/j.ijheatmasstransfer.2008.05.027